PATTERNS OF SURF-RIDING AND BROACHING-TO CAPTURED BY ADVANCED HYDRODYNAMIC MODELLING

Kostas J. Spyrou, National Technical University of Athens, k.spyrou@central.ntua.gr
Kenneth M. Weems, Science Applications International Corporation, kenneth.m.weems@saic.com
Vadim Belenky, formerly American Bureau of Shipping (ABS), vadim.belenky@navy.mil

ABSTRACT

The results of a recent research study are presented that was intended to clarify whether the numerical code LAMP could capture qualitatively phenomena of nonlinear dynamic behaviour associated with "surf-riding" and "broaching-to", for a ship that operates in extreme stern quartering seas (deterministic case). The paper includes also description and preliminary results of an implementation in LAMP of continuation analysis for surf-riding in quartering seas for all six degrees of freedom, with concurrent stability analysis.

Keywords: *ship, surf-riding, broaching-to, capsize, stability, LAMP, following sea*

1. INTRODUCTION

By-and-large, the unravelling of the dynamical basis of the surf-riding and broaching-to phenomena can be considered nowadays as a resolved issue. Yet, the achievement of satisfactory quantitative prediction of the propensity of a specific ship towards such behaviour in following/quartering seas should still be characterised as a research goal. This discrepancy is owed to the moderate confidence that we maintain about the prediction of these extreme phenomena on the basis of hydrodynamic models derived solely from first principles, without using key input from model experiments (ITTC 2005). Due to its practical worth, the topic is regarded as a challenge across the spectrum of modelling approaches (e.g. see Carrica et al. 2008).

These observations were the stimulus for undertaking collaborative research with the following specific objectives: Firstly, to verify whether an advanced hydrodynamic code, in particular the *Large Amplitude Motion Program* (*LAMP*), can reproduce the generic patterns of surf-riding and broaching, as these are described in the literature (see Spyrou 1996a, 1996c, 1997; and also their popularised descriptions in the book of Belenky & Sevastianov 2007). Secondly, to explore the possibility of incorporating into LAMP more advanced numerical techniques (i.e. to go beyond simulation) for the efficient investigation of multi-dimensional ship dynamics. Continuation analysis of surf-riding in six degrees of freedom was implemented in a "lighter" version of the code (a version that could straightforwardly attain the form of a system of ordinary differential equations). Combined with simultaneous stability analysis, this numerical environment should expedite tremendously the exploration of surf-riding in quartering seas which is believed to be closely linked with the occurrence of direct broaching. Key results from these investigations are presented below.

2. THE HYDRODYNAMIC CODES

LAMP incorporates several different formulations for the solution of the wave-body hydrodynamic interaction problem. Two of these were used for this work: LAMP-3 uses an approximate body-nonlinear 3-D, 6 d.o.f. potential flow hydrodynamic solver, especially formulated for large lateral motions. Incident wave forcing and hydrostatic restoring forces are calculated over the instantaneous wetted hull surface. Radiation and diffraction forces are calculated over the mean wetted surface; however there are no assumptions on constant forward speed and small lateral motions.

Hull lift forces are calculated considering the hull as a lifting surface of extremely low aspect ratio or using lift coefficients evaluated using another potential code VoLaR (Vortex Lattice Rationale). Vortex-shedding induced drag is modeled in a similar fashion to hull lift forces. Wave forces come naturally from the potential flow formulation.

Viscous drag force as well as yaw and sway viscous damping are implemented in a conventional way using empirical coefficients. A conventional coefficient-based model of propeller is used for thrust. As a result, forward speed is a result of calculations rather than an input figure, with the number of revolutions of a propeller as an input. A more detailed description of the force model can be found in (Lin et al. 2006).

While the LAMP-3 formulation represents a very reasonable compromise between realistic modeling and computation efficiency, the memory effect related to radiation forces does not allow a vessel to be modeled as a dynamical system described by ordinary differential equations. The implementation, at a practical level, of a continuation method requires that the dynamical system is represented as a system of ordinary differential equations. The most direct way for dealing with that for the LAMP implementation is, in the first instance, to remove the memory effect. It is noted that, for the stationary states of surf-riding that are targeted by the continuation method (to be discussed in detail later in this paper), hydrodynamic memory is not expected to change the position of stationary states in state-space, it may however have some influence (one expects not very substantial) on their stability properties. Therefore, a version of LAMP called "LAMP-0" was developed (specifically for running the continuation method – simulations were still run with LAMP-3), in which the hydrostatic and Froude-Krylov forces are evaluated on the instantaneous submerged body, while radiation forces are ignored and added mass is implemented as constant coefficient. Wave-related damping and drag forces now have to be included via external models or coefficients, in a similar fashion to viscous effects, as they are no longer evaluated directly. The maneuvering model of LAMP-3 appears intact in LAMP-0 implementation.

3. PREDICTED MOTION PATTERNS

The ship configuration used for demonstrating the surf-riding and broaching phenomena is the "tumblehome topside" form derived from the ONR Topsides Study. The ship has length $L_{WL} = 159$ m, beam $B_{WL} = 18.802$ m and maximum draught $T = 7.607$ m (Bishop, *et al.*, 2005).

A preliminary study had shown that, for a harmonic wave with wave-length-to-ship-length-ratio equal to 1.0, wave steepness 1/20; and an exactly following sea, the sample ship should exhibit surf-riding behaviour from approximately $Fn = 0.30$. From that Fn and to some distance upwards, one should anticipate the occurrence of interaction phenomena arising from the coexistence of at least two (often more) different stable conditions: the periodic state where the waves overtake the ship; and the stationary state of surf-riding ("stationary" with respect to a wave crest). In general, a higher initial surge velocity renders the capture into surf-riding more likely. (Note

on terminology: surge velocity is used here to indicate the total ship velocity in x-direction.)

Key findings are presented below for nominal *Fn* ranging from 0.3 to 0.41. The behaviour at lower speeds (*Fn* = 0.21 and *Fn* = 0.25) was also looked into; but nothing different from an ordinary response could be found for commanded headings up to 20 deg from the direction of wave propagation. Furthermore, vastly different initial conditions seemed to converge always towards the same, basically linear, response.

3.1 Main findings for *Fn* = 30

The study initially targeted changes of the periodic motion in the vicinity of the lower threshold of surf-riding; in particular, the possibility of a change in the character of the "overtaking-wave" periodic motion, manifest of the so-called "cumulative" broaching (e.g. see Conolly 1972); that has been conjectured to correspond to a scenario of "yaw resonance with a jump" (Spyrou 1997). But that had been based on a mathematical model of surge, sway, yaw and roll with the ship contouring the wave in condition of hydrostatic balance. Also, the "hydrodynamic memory" due to waves radiating from the ship had not been taken into account. One should need therefore more evidence (e.g. by trying to reproduce similar behaviour by LAMP) about the generic nature of this type of broaching.

The ship's centre of gravity was set by 1.0 m lower than the design value, in order to rule out the possibility of capsize or even the interference of nonlinear rolling. Another essential choice was, the setting of gain values for rudder's controller. In the first instance the proportional and differential gains were given the value of 3.0 (in deg per deg and deg per deg/s, respectively). No integral gain was used. For the assumed wave-length-to-ship-length-ratio, the Froude number of wave celerity is just about 0.4. Therefore, one expects the waves to be overtaking the ship. The commanded heading ψ_r was selected as the control parameter and it was varied successively from 0 to 24 deg. For each ψ_r, value at least 20 min (real-time) simulation was performed.

The change of pattern of behaviour as the commanded heading ψ_r is raised from 14 deg to 19 deg is apparent in Fig. 1. The following features are singled out from this transformation:

A gradual drop of the mean speed was realised and eventually a *quasi-periodic* pattern of response has emerged.

- The power spectrum produced on the basis of surge velocity's time series (steady-state part) shows clearly the existence of a second incommensurate period which is a very long one (over 400 s!), see Fig. 1. The emerging pattern appears like an erratic oscillation, a succession of incomplete turns. Practically, the second period is unimportant. The essential matter is the ensuing inability to maintain the course.
- Yaw was augmented, bringing about larger rudder oscillations that reached the limit of max deflection (Fig. 2a). Although the transition might not be labelled as too abrupt, it definitely points to the occurrence of a jump that should be classified as broaching.
- Heave and pitch amplitudes (Fig. 2b) have grown considerably. The transfer of energy into these modes seems to be a feature of this erratic behaviour. Hence, the observed significant drop of mean speed can be attributed to the emergence of severe horizontal and vertical oscillations.

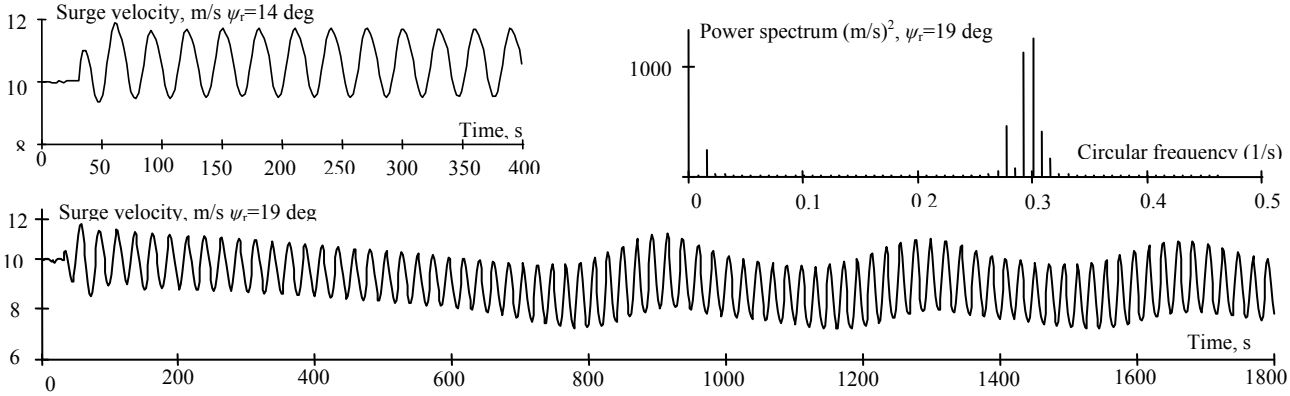

Figure 1. Fn=0.30, ψ_r=14 deg (upper left); ψ_r=19 deg (lower and upper.right).

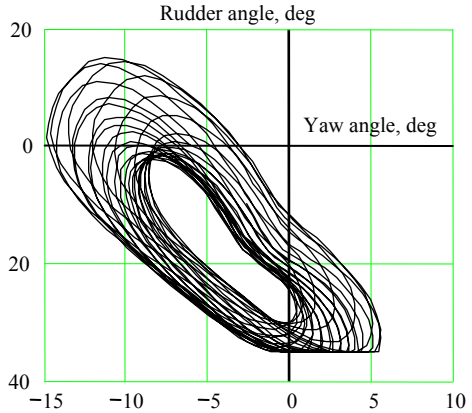

Figure 2a. Rudder angle vs. yaw angle Fn = 0.30, ψ_r = 19 deg: Very large yaw-rudder oscillation.

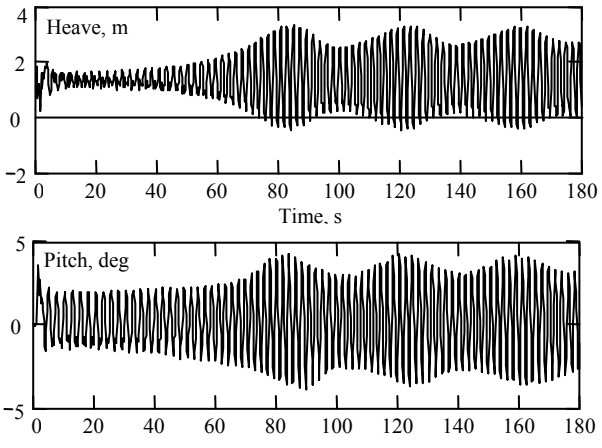

Figure 2b. Time histories of pitch and heave motions at Fn = 0.30, ψ_r = 19 deg: Growth of heave and pitch motions.

To test the sensitivity of phenomena to the intensity of control, the investigation was repeated for different gains. A very special change is shown in Fig. 3 (ψ_r =10 deg, α_ψ= 5). The frequency content of the surge response corresponds to a period-doubling event (i.e. the motion is turned sub-harmonic). Simultaneously, a substantial increase in the amplitude of yaw/rudder oscillations was realised, a typical consequence of this type of bifurcation. Increase of the commanded heading to ψ_r = 16 deg gave rise to the jump towards quasi-periodic response. However, the yaw-rudder oscillation had already become large prior to the jump. The realised drop of mean speed is in this case associated mostly with transfer of energy into heave and pitch with subsequent growth of these vertical plane motions. Obviously, the higher gain restricted the yaw/sway oscillations (adding to this, the sway velocity did not show any significant change before and after the jump).

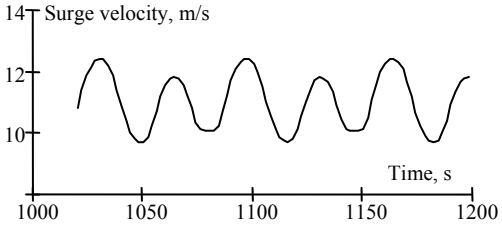

Figure 3. Sub-harmonic surging (Fn=0.30, ψ_r=10 deg, a_ψ=5).

A summary of the observed motions, as ψ_r is raised, is presented in Fig. 4.

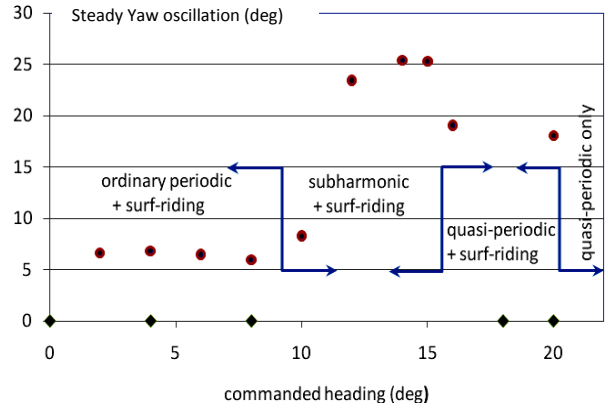

Figure 4. Summary of observed types of behaviour at $Fn = 0.3$ as function of commanded heading.

3.2 *Fn* = 0.33

In Fig. 5 is shown a summary of the responses (for a nominal speed of $Fn = 0.33$) as characterised by their steady amplitude. It was necessary to repeat many of these runs from different initial surge velocities, in order to capture the coexistence of surf-riding and periodic motion. At ψ_r just above 10 deg, the "edge" of the surf-riding domain is reached. The escape from surf-riding that occurs when this boundary is crossed outwards is a jump phenomenon, leading abruptly back to the domain of "overtaking-waves" periodic motions. Initially, these appear as ordinary asymmetric (nonlinear) responses at the frequency of encounter. However, with a further increase of the commanded heading they turn into sub-harmonic response. It is remarkable that a further increase of ψ_r invoked a return to the ordinary periodic response for commanded headings at least up to $\psi_r = 20$ deg.

Sometimes an interesting phenomenon appeared where a higher gain value gave rise to periodic surging while a lower gain lead to surf-riding (Fig. 6). Considering the time histories of surge and yaw (not shown here), it is quite intriguing that, despite the very little difference at the initial part of the response, qualitatively different patterns eventually resulted.

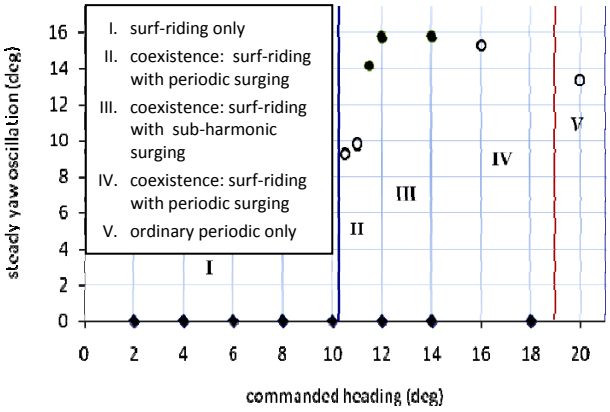

Figure 5. Summary of observed types of behaviour at $Fn = 0.33$ as function of commanded heading.

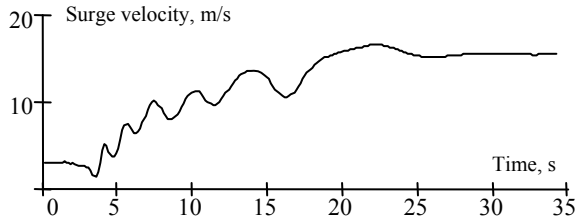

Figure 6a. Convergence to surf-riding for $\psi_r = 4$ deg, $a_\psi = 3$.

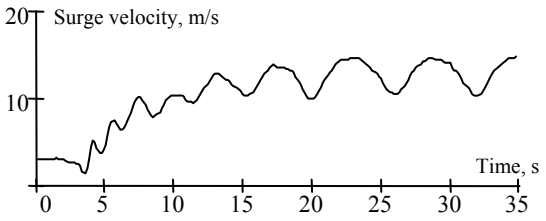

Figure 6b. Convergence to periodic surging for $\psi_r = 4$ deg, $a_\psi = 5$.

3.3 Fn = 0.36

A remarkable feature that appeared at this higher nominal speed was a stable oscillatory type of surf-riding, residing at the outskirts (in terms of commanded heading) of the domain of surf-riding (Fig. 7). As the ship is carried along by a single wave, it is also oscillating in all directions on the wave's down-slope. This fascinating occurrence has been observed in the past and it was explained as being due to a

Hopf bifurcation (Spyrou 1996a). It is known that the differential gain governs the onset of this behaviour. Oscillations emerged at ψ_r about 9 deg. The frequency content for one scenario of oscillatory surf-riding can be deduced from the power spectrum shown in Fig. 8b. Distortion from the harmonic pattern (Fig. 8a) is noticed, due to higher harmonics, most prevalently the 2ω harmonic. Sometimes, oscillatory surf-riding was found to coexist with the "overtaking-wave" periodic motion.

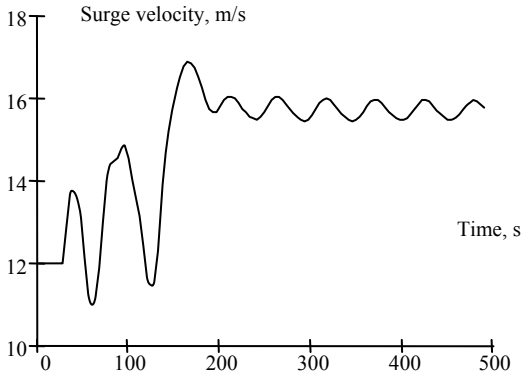

Figure 7. Capture into oscillatory surf-riding for ψ_r = 12 deg, $a_\psi = 3$ (notice the upward jump of mean speed).

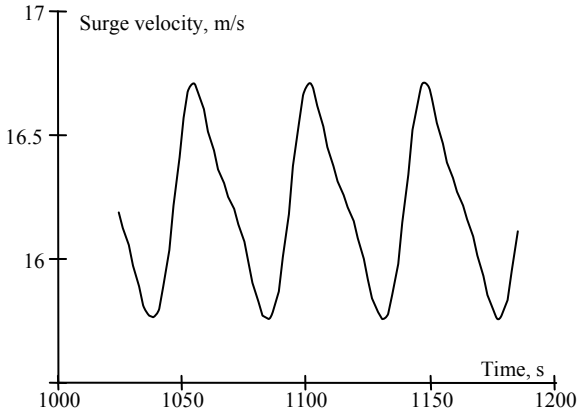

Figure 8a. Oscillatory surf-riding with second harmonic influencing the motion (steady state) $\psi_r = 17.9$ deg, $a_\psi = 3$.

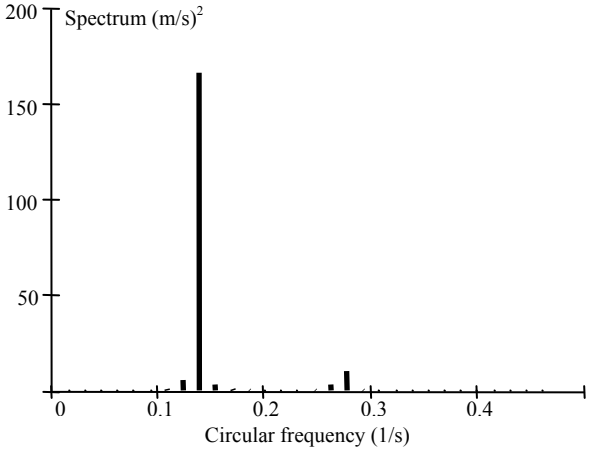

Figure 8b. Power spectrum of oscillatory surf-riding with second harmonic influencing the motion; $\psi_r = 17.9$ deg, $a_\psi = 3$.

3.4 *Fn* = 0.38 *and* *Fn* = 0.41

The final two nominal speeds were selected in the vicinity of wave celerity. In that region even period-doubled surf-riding oscillations emerged. Their nature and domain of existence have also been discussed in the past (Spyrou 1996b). A characteristic transition from period-doubled oscillatory surf-riding towards the ordinary overtaking wave response can be seen in Fig. 9. At such a large commanded heading value, oscillatory surf-riding could not be sustained for long and the ship inevitably escaped from surf-riding.

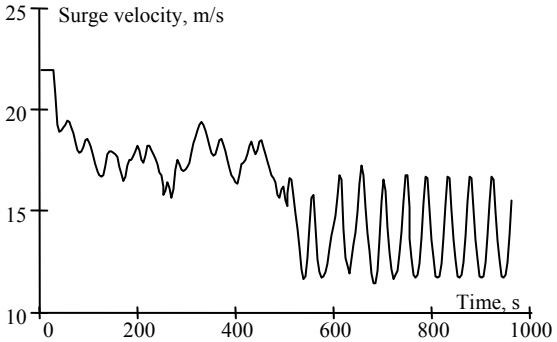

Figure 9. Escape from period-doubled oscillatory surf-riding towards ordinary "overtaking-wave" periodic motion ($Fn = 0.41$, $\psi_r = 28$, $a_\psi = 3$).

3.5 Summary of the simulation study

The domain of nominal Froude numbers and commanded headings where surf-riding appeared has been summarised in Fig. 10.

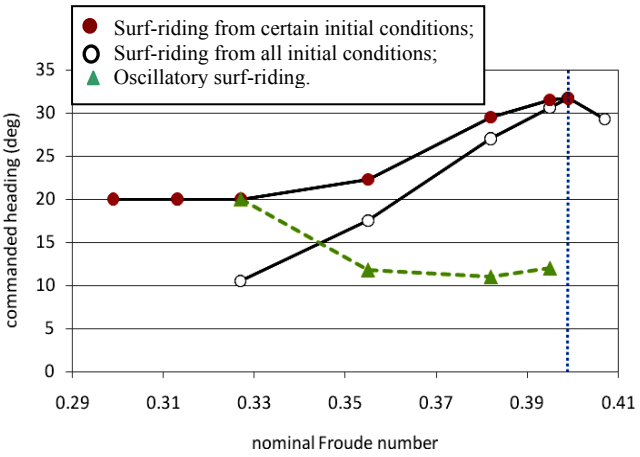

Figure 10. Boundaries of surf-riding in terms of commanded heading as a function of nominal Froude number.

4. THE CONTINUATION SCHEME

The continuation code DERPAR which had been used by the first author for investigating surf-riding and broaching, was interfaced with a subroutine-based version of LAMP's force calculation routines, under a new top level supervisory code. The resulting code was named LAMPCont. Some background details of this implementation are given below.

Consider the mathematical model of a ship that moves in quartering seas, brought into the following generic ODE form:

$$\dot{\mathbf{x}} = \mathbf{f}\left(\mathbf{x};\boldsymbol{\alpha};t\right) \qquad (1)$$

$\mathbf{x}$ is the state vector; $\boldsymbol{\alpha}$ is the control parameters' vector which could include real controls as well as parameters that represent the environment. As usual, t is the time. Strictly speaking, bringing ship motion equations to form (1) may not be possible without having to deal with an essentially infinite number of ODEs. For an observer that moves with the wave, ordinary surf-riding should correspond to the stationary states of (1). These could be identified if, the explicit time dependence was removed from (1); and then request all components of the velocity vector to be zero. Then (1) should become:

$$\mathbf{f}\left(\mathbf{x};\boldsymbol{\alpha}\right) = 0 \qquad (2)$$

Removal of the direct time dependence is possible for the pressure-related terms for which ship's position in waves, rather than time, is the key factor in the calculation; but it may not be trivial for perturbation/radiation terms which are in fact responsible for the infinite dimensional nature of the ship motions problem. The applicability of continuation in the current context seems thus to be dependent on how important these terms are, for the specific scenarios that are investigated; and if they are, whether some reasonable low-dimensional approximations of these could be produced.

The right hand side (RHS) vector $\mathbf{f}$ is a function of the external forces, the mass and mass moments of inertia, the kinematic relationships between the derivatives of the position vector and velocity, and (if necessary) control or servo models. Continuation searches for the locus of solutions $\mathbf{x}$ and $\boldsymbol{\alpha}$ that satisfy the relationship expressed by equation (2). These points represent solutions where the time derivatives of the state variables are zero, so they are equilibria, although not necessarily stable ones. These equilibria are found by performing an initial search for a single equilibrium point and then tracking the curves of equilibria through the solution domain. The name continuation derives from the "continuous" nature of this tracking and the locus of solution points. The key quantity in this search is the Jacobian matrix $\mathbf{J}$, which represents the derivatives $\mathbf{f}$ with respect to both the state and control vectors, $\frac{\partial}{\partial x_i}\mathbf{f}(\mathbf{x};\boldsymbol{\alpha})$, $\frac{\partial}{\partial a_j}\mathbf{f}(\mathbf{x};\boldsymbol{\alpha})$. One of the key aspects of the continuation formulation is that

the RHS vector **f** and the Jacobian **J** must be explicitly computed from the state vector **x**, control setting $\boldsymbol{\alpha}$, and data such as the sea conditions, hull geometry, etc. In its current state, the analysis does not allow for a "memory" effect where the forces acting on the ship are dependent on the history of how the ship got to its current position.

Key parts of creating LAMPCont were:

- re-implementing LAMP's equations of motion (EOM) in diagonalized form suitable for continuation;
- evaluating the right-hand-side (RHS) vector **f** using the LAMP force calculation;
- evaluating the Jacobian matrix **J**.

The first of these parts was based on LAMP's standard 6-DOF formulation of the equations of motion (Lin and Yu, 1990, 1993). The second part of the implementation was to evaluate the RHS vector **f** using the LAMP force calculation. This involved three steps:

- Transform the continuation state vector x to the LAMP state variables and transform the control vector $\boldsymbol{\alpha}$ to the corresponding LAMP variables.
- Calculate forces/moments on the ship using a subroutine implementation of LAMP.
- Calculate **f** from the EOM using the force returned by the LAMP subroutine, the mass and mass moment of inertia, and an estimate for the added mass.

The subroutine-based implementation of LAMP uses exactly the same subroutines as a regular LAMP simulation at each time step. This force calculation includes the body-nonlinear hydrostatics and Froude-Krylov pressure forces; appendage forces due to rudders, bulge keels, and skegs; propeller force; manoeuvring forces such as hull lift; and approximate viscous force models. Because the force must be computed explicitly in terms of the state and control variables, this force does *not* include components associated with the hydrodynamic perturbation potential of the wave-body interaction problem such as radiation or diffraction. As a result, the implementation corresponds to the LAMP-0 or "hydrostatics & F-K only " model.

A third key part of the implementation is the calculation of the Jacobian matrix **J**. In the present implementation, this is done by setting-up "variant" state vectors with some perturbation of each state or control variable in turn, computing the RHS vector for the variant states, and estimating the derivatives via a finite difference scheme:

$$\mathbf{x}_V = \mathbf{x} + \Delta x_i$$

$$\frac{\partial}{\partial x_i}\mathbf{f}(\mathbf{x};\boldsymbol{\delta}) \cong \frac{\mathbf{f}(\mathbf{x}_V;\boldsymbol{\delta}) - \mathbf{f}(\mathbf{x};\boldsymbol{\delta})}{\Delta x_i} \qquad (11)$$

An additional piece of the LAMPCont implementation was to integrate standard math library routines for the Eigenvalue and Eigenvector calculation. This is essential for performing stability analysis at each identified surf-riding state. The structure of the LAMPCont program is shown in Fig. 11.

The input to LAMPCont includes:

- LAMP input control file defining the geometry, appendages, and other LAMP data.
- Initial values, upper and lower limits, and perturbation increments for a Jacobian calculation for each state and control variable.
- Additional problem-dependent definitions such as wave height and length, and settings for control parameters that are not being varied in the Continuation analysis.
- Continuation controls such as step size limits and number of points.

LAMPCont's principal output consists of the locus of equilibria solution points and the eigenvalues and eigenvectors of the Jacobian at the solution points. The following problems have been implemented in LAMPCont:

- Surf-riding in following seas, 3-DOF (surge, heave, pitch) vs. propeller speed.
- Turn in calm water, 3-DOF (surge, heave, yaw) vs. rudder.

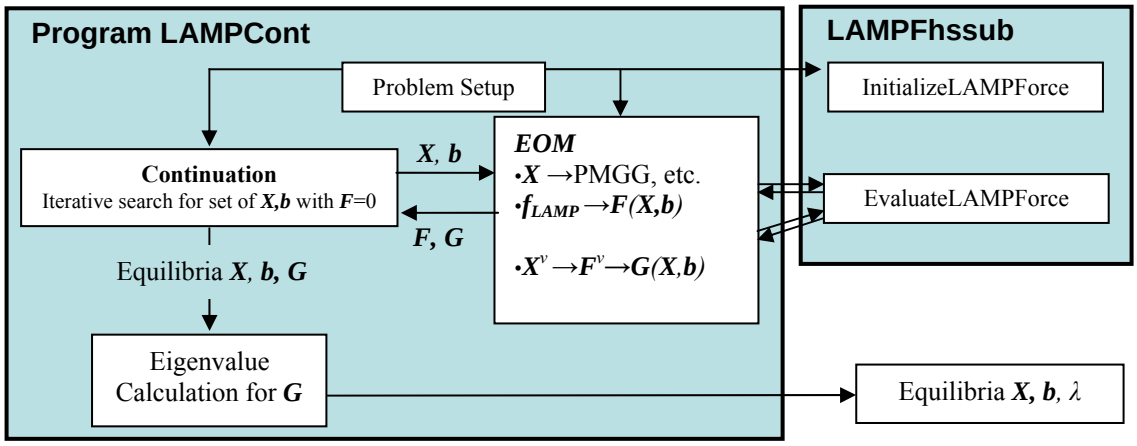

Figure 11. Structure of LAMPCont.

- Turn in calm water, 6-DOF vs. rudder.
- Surf-riding in following/quartering seas, 6-DOF vs. rudder (unsteered).
- Surf-riding in following/quartering seas, 6-DOF vs. commanded heading (autopilot).
- Surf-riding in following/quartering seas, 6-DOF vs. commanded heading (autopilot + servo equation).

The turning problems were initially implemented primarily as successively more complicated tests of LAMPCont, but may prove to be very useful in analyzing the characteristics of LAMP's "manoeuvring" force models, both in an overall modelling sense and for ship-specific model input.

As part of the LAMPCont development, a specialized graphics-tool called PltCont has been developed to plot LAMPCont results, including projections of the solutions and eigenvalues loci.

4.1. What about the hydrodynamics?

As mentioned, the present formulation of the continuation analysis requires a "point" evaluation of $\mathbf{f}(\mathbf{x};\boldsymbol{\alpha})$, which precludes LAMP's regular time-domain evaluation of the wave-body hydrodynamic disturbance, including the effects of radiation, diffraction, etc. As a result, this initial implementation corresponds to LAMP-0, or a "hydrostatics-only" modelling, with relatively minimal accounting for additional hydrodynamic effects, such as a constant added mass coefficient. The impact of this issue cannot yet be evaluated and will be a principal objective as the project continues. However, some points have been identified.

Within a LAMP-3 simulation, the current LAMP-0 implementation may well be adequate for identifying the "distance" of the ship to the equilibrium boundaries, although this is primarily conjecture at this point. However, the hydrodynamic effects related to radiation should be small at the point of equilibrium, since the ship motion must match the motion of the wave. Diffraction and

forward speed effects may well be important, but can, in principle, be estimated for: a) the values from the current simulation (i.e. point from which we are measuring the distance) or, b) a pre-computed approximate hydrodynamic solution based on the ship's travelling at an equilibrium point.

In addition, the LAMP-0 implementation of LAMPCont is likely to be more than adequate for assessing force models, especially those related to propulsion and manoeuvring. If the disturbance hydrodynamics do seem to be important, several approaches can be investigated to better incorporate them, such as:

- Impulse response function (IRF) like expressions for disturbance potentials (especially diffraction), "linearized" about $u = V_{\text{wave}}$.
- Variation to instantaneous time-domain solution (for distance to boundary).
- Expanded Continuation scheme with memory effect using some kind of state space approximation, developed from theoretical models or characterization of LAMP simulation results.
- Expanded ODE-like terms with constant or state-dependent coefficients.

5. SAMPLE LAMPCont RESULTS

LAMP-based continuation analysis was applied for several surf-riding and ship turning problems. Preliminary testing and evaluation of LAMPCont appears to show that results are self-consistent, in that the stable equilibrium solutions can be reproduced via direct simulation. They also seem reasonable, in that they qualitatively match the results of continuation analysis of theoretical models. A few sample results are shown below.

5.1 3-DOF surf-riding in following seas

The simplest problem that has been implemented in LAMPCont is surf-riding in following seas, solving for an equilibrium in surge, heave, and pitch as a function of propeller speed in revolutions per second (RPS). Fig. 12 shows a typical result for the sample ship in a wave that is 200 m long and 4 m high. In this analysis, the ship has 2 propellers which are modelled using a specified K_T curve derived from a generic B-series propeller.

The main left hand plot is a projection of the equilibria solution locus showing the position of the ship's centre of gravity relative to the wave crest. In this plot, $X = 0$ and 200 correspond to the ship on the wave crest, $X = 100$ is at the wave trough, and $X = 50$ is halfway down the face of the wave. The curve shows that, for this wave, there is both a lower and upper limit of the propeller speed for which a surf-riding equilibrium can be found, below which the wave cannot supply enough extra force to propel the ship at the wave celerity and above which the wave cannot provide enough retarding force to slow the ship to wave celerity. For points in between, there are two equilibria.

The two equilibria are marked for a propeller rate of 3.0 RPS, which corresponds to the calm water self-propulsion speed just below the wave celerity. The two equilibria are on the down-slope of the wave, just below the crest and just above the trough. The inset plots on the left show the eigenvalues at the two points, which indicate that the point near the crest is an unstable equilibrium while the point near the trough is stable. The right hand plot shows projections for the heave motion (+ *down* relative to calm water flotation) and pitch (+ *bow up*) of the locus of equilibrium points. These results seem quite reasonable and agree well with previous theoretical analysis of the surf-riding in following seas.

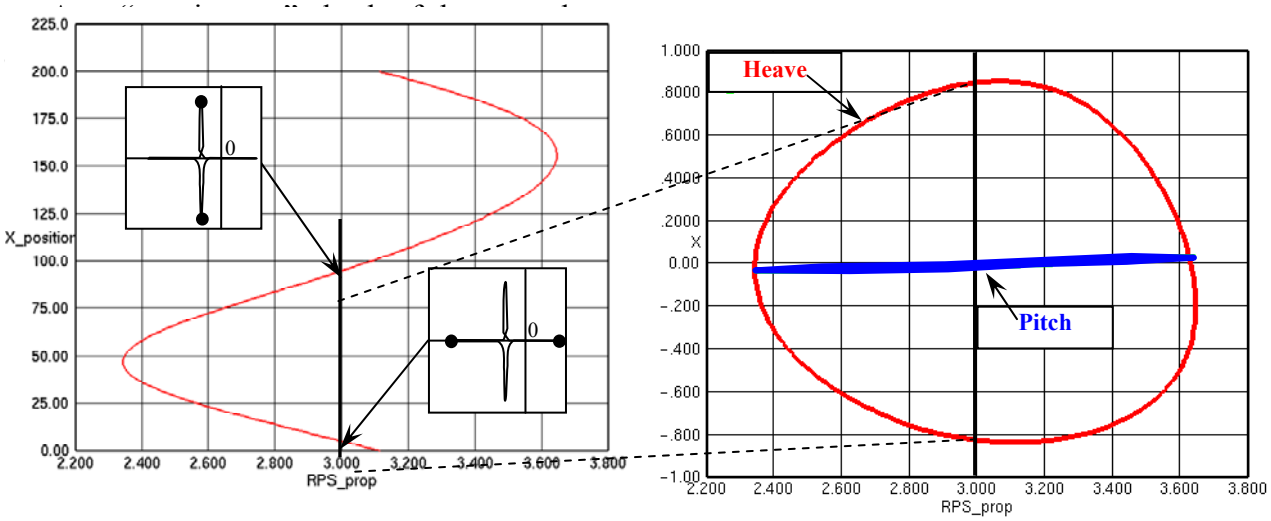

Figure 12. LAMPcont result for surf-riding in following seas.
Eigenvalues loci are shown in the insets.

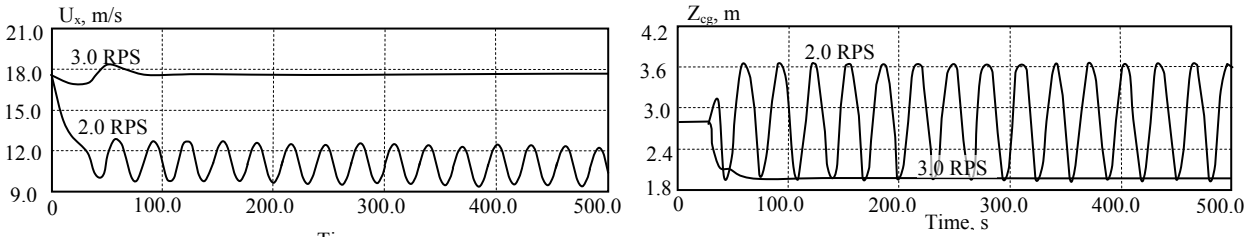

Figure 13. Time histories of velocities: simulations with LAMP-0 at two different propeller rates.

Figure 13 shows time histories of ship velocity (left graphs) in the direction of the wave propagation and heave motion (right graphs) defined by the vertical position of the centre of gravity *wrt* the mean water surface, for two propeller speeds. In both cases, the ship starts with a speed close to wave celerity, so a surf-riding equilibrium is likely to be reached if one exists. At the lower propeller rate (2.0 RPS), for which the continuation analysis indicated there was no stable surf-riding equilibrium, the ship slows to oscillatory surging. At the higher rate (3.0 RPS), the ship transitions to surf-riding at a point near the wave trough, with steady heave and pitch values that match those predicted by LAMPCont.

5.2 6-DOF surf-riding in stern oblique seas

Three different versions of the problem of 6-DOF surf-riding in long-crested following or stern quartering seas have been implemented:

- Unsteered ship with specified rudder deflection.
- Steered ship with specified commanded heading and PD autopilot.
- Steered ship with specified commanded heading, PD autopilot and rudder servo.

In the LAMPCont implementation of the 6-DOF surf-riding problems, the displacement and velocities of all 6 rigid body motions are solved for, *except* for ship's position along the crest of the wave (global Y

coordinate), which can have a non-zero but constant velocity at equilibrium.

For the unsteered ship, the rudder deflection angle is the control parameter in the continuation calculation. For the steered ship, the command heading angle is the control parameter and PD rudder control is applied. Two steered ship models have been implemented. In the first, the rudder deflection is explicitly set based on the heading angle and yaw rate. This model assumes instantaneous rudder response. In the second, a servo lag term in introduced and the deflection of the rudder is now computed using a servo equation that is solved simultaneously with the equations of motion.

Note that the rudder deflection must be constant at the equilibrium points (by the definition of equilibrium, its derivative must be zero like the state variables), so the introduction of the servo equation should not change the computed equilibria. It can, however, change the force derivatives and hence the stability of the equilibria, which can be seen by the eigenvalues of the Jacobian matrix. In a similar fashion, the gains of the PD rudder control will not affect the equilibria but will affect their stability.

6-DOF surf-riding continuation analysis was performed in stern seas for the sample ship, with varying degrees of directional stability. This was varied by imposing artificially a change in the longitudinal position of hull lift (effectively changing the turning moment due to hull lift) and the size of the bilge keels, skeg, and rudders on the computational model.

Fig. 14 shows some results for the stability variants with a fixed propeller speed of 3.0 RPS in a wave with that is 200 m long and 4 m high. The upper plot shows the ship's yaw angle relative to the wave direction (in radians) *vs.* the rudder deflection angle (in degrees). A yaw angle of 0.0 corresponds to pure following seas. The lower plot shows the position of the ship on the wave as the distance from the wave crest to the CG. As the ship gets less and less stable, a larger rudder deflection is required to maintain a large angle relative to the wave.

While a few self-consistency checks have been performed, the primary check should be to compare them with the theoretical evaluations described in previous continuation work. Fig. 15 shows the yaw *vs.* rudder equilibrium solution loci for two of the stability variations along with a drawing of similar nature for a fishing vessel that had been obtained earlier (Spyrou 1996).

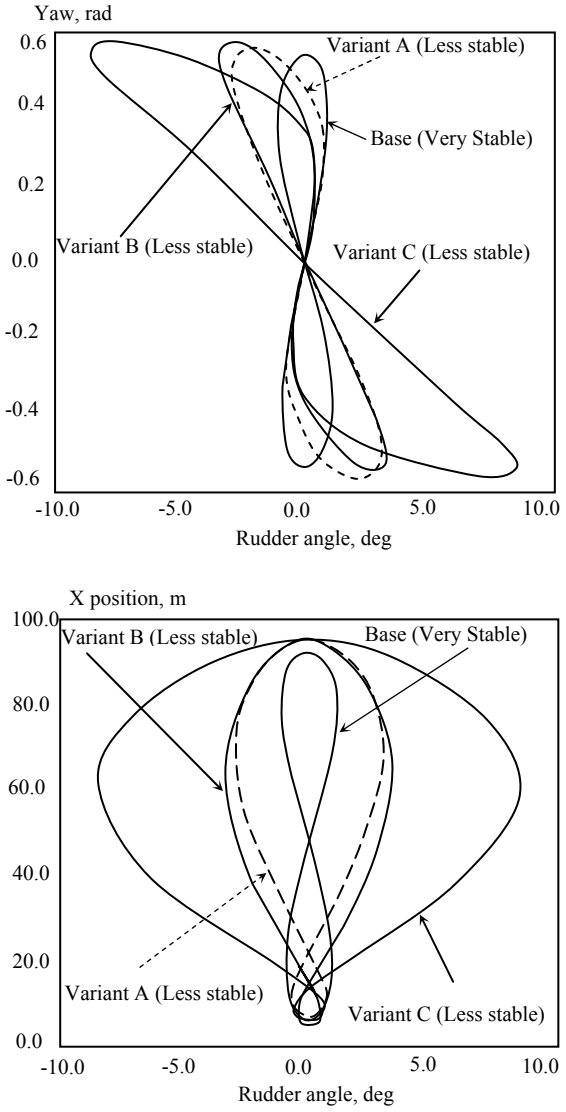

Figure14. Output of LAMPCont for the sample ship in queartering seas.

The results are qualitatively very similar including the occurrence of a Hopf bifurcation, which can be identified by the position of the eigenvalues in the inset plots of the LAMPCont results.

Fig. 16 shows initial results for ship with autopilot in the 4m wave, again at a propeller rate of 3.0 RPS. These results show that the surf-riding equilibrium heading for the stable ship is very close to the command heading, while the less stable variants are seeing a larger and larger error in the realized *vs.* command course. Fig. 17 shows similar results for the larger wave height of 6m. For the least stable variants, a small commanded heading can induce a very large yaw angle. The right-hand plot shows the rudder angles associated with the equilibrium solutions. There is a slight "hitch" in the curve for the most unstable case, which appears to be a result of the stall of the hull or appendage lift due to very large sideslip angle. By default, the LAMP lift model is discontinuous at this point, with the lift expression abruptly replaced by an empirical "eddy-making" model. Despite this discontinuity in a principal force mode, the Continuation method was able to track the equilibrium solution locus through this region. This calculation was repeated with the servo model. However, the solution locus was found to be the same with and without the servo model, which is exactly what was expected.

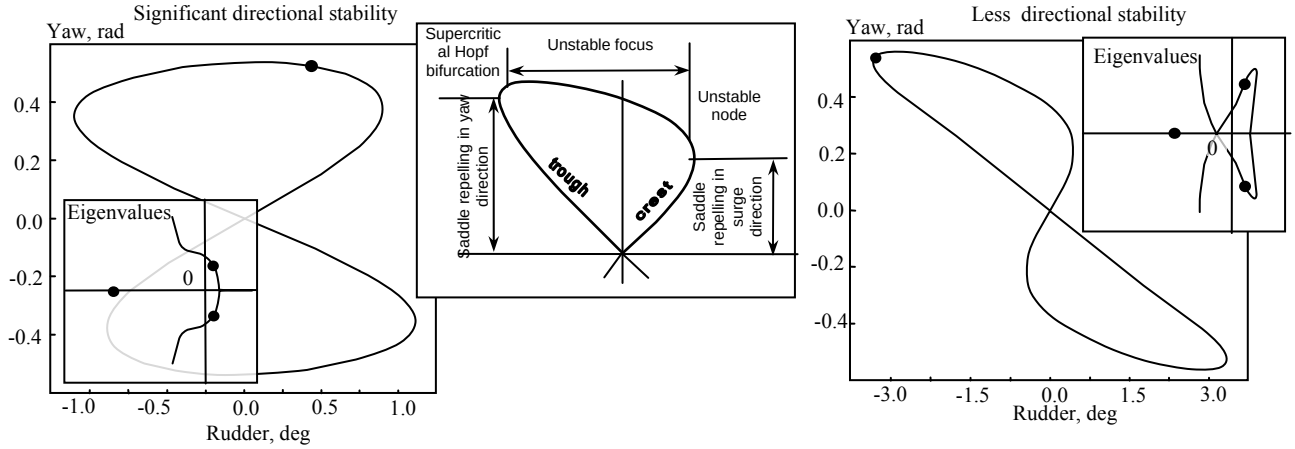

Figure 15. Layout of surf-riding equilibria for two sample variants (left and right) and contrast with pre-existing similar graph for fishing vessel (center).

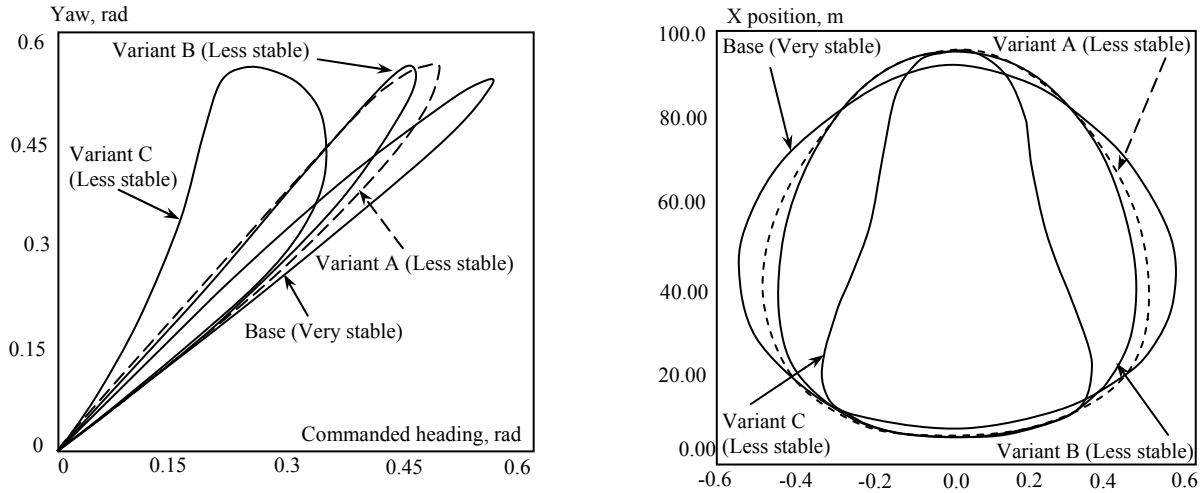

Figure 16. LAMPCont results with autopilot included.

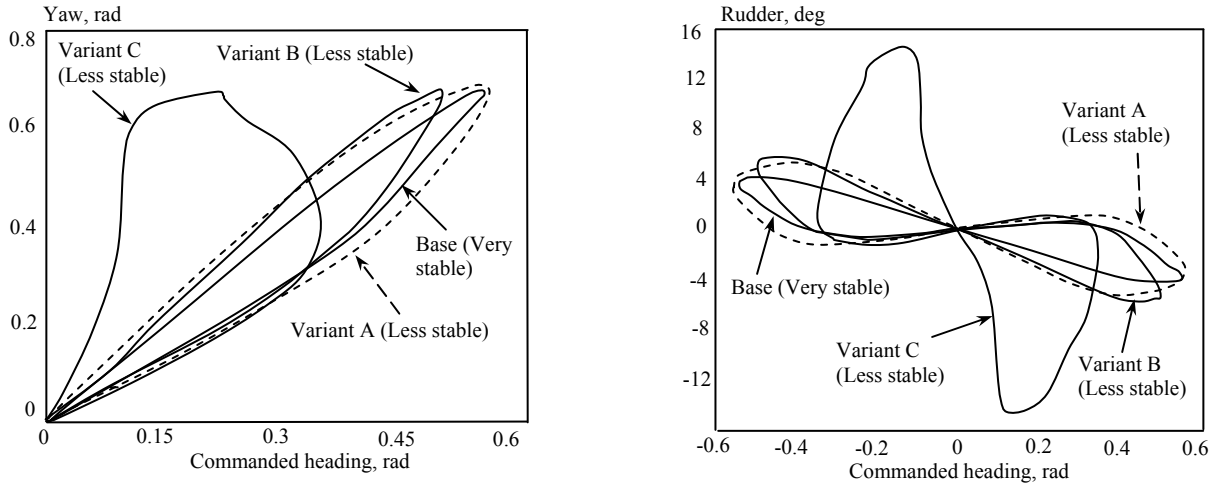

Figure 17. LAMPCont results with autopilot and larger wave height.

6. CONCLUSIONS

Behaviour that is consistent with the current theory of broaching and surf-riding has been reproduced by targeted LAMP simulations, for a tumblehome-topside ship. Besides the fact of taking the step of investigating these strongly nonlinear phenomena of ship behaviour by an advanced numerical code of ship hydrodynamics, the result is important for the extra reason that, it corroborates the generic nature of the phenomena that had been identified independently and for a very different configuration in earlier research. Furthermore, the capture into surf-riding in quartering seas, as well as the escape from it, taking into account all six degrees of freedom of ship motion, has been studied at a preliminary level.

Continuation analysis has been successfully integrated with a subroutine-based force calculation to produce a LAMP-based continuation analysis code called LAMPCont. While some technical issues in the equilibria tracking remain to be resolved, the basic implementation has been shown to be consistent with direct simulation of the stable equilibria as well as the results of previous continuation research of a more theoretical nature. However, this formulation of the continuation approach does not allow for memory in the calculation and has therefore prevented the inclusion of the full LAMP-based hydrodynamic calculation. As a result, the current implementation is based on the LAMP-0 or "hydrostatic-only" model of wave-body hydrodynamics.

With this basic implementation of the continuation approach completed, future work will focus primarily on investigating and possibly mitigating the effects of the hydrodynamic model approximations and the application of the continuation approach to the characterization of surf-riding and broaching, with the goal being to predict a probability of surf-riding and broaching in irregular waves and an evaluation of the risk of such phenomena leading to extreme roll motion including capsizing.

7. ACKNOWLEDGMENTS

The work described in this paper has been funded by the Office of Naval Research under Dr. Patrick Purtell.

This work was carried out during the first author's stay at the American Bureau of Shipping (ABS) in Houston, on sabbatical leave from the National Technical University

of Athens (NTUA). The authors spent several productive days together at Houston, as well as at the Offices of Science Applications International Corporation (SAIC) in Bowie. The authors thank the two Organisations for their support and for their hospitality.

The development of the LAMP System has been supported by the U.S. Navy, the U.S. Defense Advanced Research Projects Agency (DARPA), the U.S. Coast Guard, ABS, and SAIC.

The authors are grateful to Arthur M. Reed for a detail review that improved readability of the paper. The help of Julia Belenky with the figures is greatly appreciated.

8. REFERENCES

Belenky, V.L. & Sevastianov, N.B. (2007) Stability and Safety of Ships: Risk of Capsizing. SNAME, Jersey City, ISBN 0-939773-61-9.

Bishop, B, Belknap, W., Turner, C., Simon, B., Kim, J. (2005) Parametric Investigation on the Influence of GM, Roll Damping, and Above-Water Form on the Roll Response of Model 5613, Report NSWCCD-50-TR-2005/027, Naval Surface Warfare Center/Carderock Division, West Bethesda, Maryland.

Carrica, P.M., Paik, K.J., Hosseini, H.S. & Stern, F. (2008) "URANS analysis of broaching event in irregular quartering waves" J. Marine Science & Technology, Vol. 13, No 4, pp. 395-407.

Conolly, J.E. (1972) Stability and control in waves: a survey of the problem. *Proc. of Int. Symposium on Directional Stability and Control of Bodies Moving In Water*. *J. of Mechanical Science* 14(7), (Supplementary Issue), pp. 186–193.

ITTC (2005) Report of Specialist Committee on Stability in Waves, Edinburgh.

Lin, W.M., and Yue, D.K.P. (1990). Numerical Solutions for Large-Amplitude Ship Motions in the Time-Domain *Proceedings of the Eighteenth Symposium of Naval Hydrodynamics*, The University of Michigan, U.S.A.

Lin, W.M., and Yue, D.K.P. (1993). Time-Domain Analysis for Floating Bodies in Mild-Slope Waves of Large Amplitude, *Proceedings of the Eighth International Workshop on Water Waves*

Lin, W.M., Zhang, S., Weems, K. & Luit, D. (2006) Numerical simulations of Ship Maneuvering in Waves, Proceedings of 26th Symposium on Naval Hydrodynamics, Rome, Italy.

Spyrou, K.J. (1996a) Dynamic instability in quartering seas: The behavior of a ship during broaching, Journal of Ship Research, SNAME, 40, No 1, 46-59.

Spyrou, K.J. (1996b) Homoclinic connections and period doublings of a ship advancing in quartering waves (1996). CHAOS: An Interdisciplinary Journal of Nonlinear Science, American Institute of Physics (AIP), 6, No. 2, 209-218.

Spyrou, K.J. (1997) Dynamic instability in quartering seas-Part III: Nonlinear effects on periodic motions. Journal of Ship Research, SNAME, 41, No 3, 210-223.